

Influence of template type and buffer strain on structural properties of GaN multilayer quantum wells grown by PAMBE, an x-ray study

This article has been downloaded from IOPscience. Please scroll down to see the full text article.

2011 J. Phys. D: Appl. Phys. 44 025403

(<http://iopscience.iop.org/0022-3727/44/2/025403>)

[View the table of contents for this issue](#), or go to the [journal homepage](#) for more

Download details:

IP Address: 194.44.242.242

The article was downloaded on 17/12/2010 at 06:40

Please note that [terms and conditions apply](#).

Influence of template type and buffer strain on structural properties of GaN multilayer quantum wells grown by PAMBE, an x-ray study

**V P Kladko¹, A V Kuchuk¹, N V Safryuk¹, V F Machulin¹, P M Lytvyn¹,
V G Raicheva¹, A E Belyaev¹, Yu I Mazur², E A DeCuir Jr^{2,3}, M E Ware²,
M O Manasreh³ and G J Salamo²**

¹ V. Lashkaryov Institute of Semiconductors Physics, NAS of Ukraine, Kyiv 03028, Ukraine

² University of Arkansas, Department of Physics, Fayetteville, AR 72701, USA

³ University of Arkansas, Department of Electrical Engineering, Fayetteville, AR 72701, USA

E-mail: kladko@isp.kiev.ua

Received 5 September 2010

Published 16 December 2010

Online at stacks.iop.org/JPhysD/44/025403

Abstract

The influence of template type and residual strain of the buffer layer on the structural properties of GaN/AlN superlattices (SLs) was studied using high resolution x-ray diffraction. Using sapphire substrates, an effective thinning of the GaN quantum wells and the corresponding thickening of the AlN barriers were observed in SL structures grown on thin, strained AlN templates as compared with SL structures grown on thick, relaxed GaN templates. Moreover, a bimodal strain relaxation of SL structures in dependence of template type was observed. The SLs grown on AlN templates relax predominantly by the formation of misfit dislocations, while the SLs grown on GaN templates relax predominantly by cracking of the layers. We explain these effects by the influence of residual strain in the buffer/template systems used for the growth processes of SL layers. A correlation is made between the strain state of the system and the cracking processes, the dislocation density, the radius of curvature and the layer thickness.

(Some figures in this article are in colour only in the electronic version)

1. Introduction

Heterostructures based on III-nitrides have great potential for application in optoelectronics (UV-photodetectors, light emitting and laser diodes) as well as in electronics (high-speed switches, high-temperature and high-current transistors) [1]. GaN/Al(Ga)N superlattices (SLs) have become important as the active elements in many of these devices.

In recent years, great efforts have been made to understand the nature of heteroepitaxial growth of GaN/AlN SLs using various methods [1–6], because the efficiency of GaN/AlN-based devices is limited by their structural perfection, e.g. quality of the interfaces, densities of dislocations (10^9 – 10^{10} cm $^{-2}$), etc. In fact, the dependence of the interface abruptness in GaN/AlN multiquantum wells

(MQWs) grown by metal-organic vapour chemical deposition (MOCVD) on the growth temperature was reported earlier [5], and it was concluded that lower temperatures favour abrupt GaN/AlN interfaces. The effect of growth on the performance of Si-doped GaN/AlN MQWs grown by plasma-assisted molecular beam epitaxy (PAMBE) for intersubband optoelectronics was studied in [6]. A commonly observed feature is the presence of multiple peaks in both intersubband absorption and interband emission spectra, which are attributed to thickness fluctuations in the quantum wells, induced by dislocations and eventually by cracks or metal accumulation during the growth.

In general, it has been established that the growth of the nitride layers can be two dimensional (Frank–van der Merwe 2D growth mode) [7] with slow plastic relaxation

Table 1. Structural parameters of GaN/AlN SLs grown on the GaN and AlN templates obtained from the XRD data (experimentally measured value (data obtained as a result of fitting)/technological parameters).

Samples	d_{GaN} (nm)	d_{AlN} (nm)	T (nm)	$\varepsilon_{zz} (\times 10^{-2})$	$\varepsilon_{\text{aver.}} (\times 10^{-2})$	$N_{\text{cracks}} (\times 10^2 \text{ cm}^{-1})$
<i>GaN template</i>						
NB 165	$1.70 \pm 0.07/1.98$	$2.30 \pm 0.06/1.98$	$4.00 \pm 0.03/3.96$	0.434 ± 0.002	-2.469	4.0
NB 166	$1.23 \pm 0.07/1.59$	$2.18 \pm 0.07/1.98$	$3.41 \pm 0.02/3.57$	-0.037 ± 0.002	-2.602	15
NB 157	$1.90 \pm 0.06/1.98$	$2.16 \pm 0.06/1.98$	$4.06 \pm 0.02/3.96$	0.399 ± 0.002	-2.214	8.0
NB 158	$1.85 \pm 0.07/2.06$	$2.08 \pm 0.06/1.98$	$3.93 \pm 0.04/4.04$	0.003 ± 0.002	-2.200	16
<i>AlN template</i>						
NB 148	$1.60 \pm 0.04/2.06$	$2.48 \pm 0.07/2.05$	$4.08 \pm 0.01/4.11$	0.268 ± 0.002	-2.431	0.2
NB 151	$1.50 \pm 0.04/1.98$	$2.50 \pm 0.05/1.98$	$4.00 \pm 0.01/3.96$	0.355 ± 0.002	-2.393	0.4
NB 152	$0.94 \pm 0.05/1.49$	$2.45 \pm 0.04/1.98$	$3.39 \pm 0.02/3.47$	0.115 ± 0.002	-2.891	1.0

and three dimensional (Stranski–Krastanow 3D growth mode) [8] with elastic relaxation, independent of the growth temperature/pressure and V/III ratio. The process of strain relaxation in GaN/AlN SLs not only depends on the growth mode but also depends on the type of substrate, due to the lattice mismatch-induced stress. There are different possible ways to relax the misfit-induced strain in the epilayer: (i) elastic strain relaxation by an undulation of the surface or by twist of cells of the epilayer with respect to the cells of the substrate [9] or (ii) plastic strain relaxation by crack propagation or decohesion of the layer and introduction of misfit dislocations [10].

The misfit relaxation mechanisms in short-period GaN/AlN SLs grown by PAMBE on GaN or AlN templates were analysed in [11]. The initial misfit relaxation in the vicinity of the buffer occurs by the formation of α -type dislocations. It was established, however, that using excess Ga reduces the free surface energy in the (0001) plane minimizing the strain relaxation for both the GaN and the AlN layer. The presence of cracks in these structures has not been observed. Ultimately, however, after ~ 10 –20 periods of the SL, the final strain state is independent of the template type (GaN or AlN). Periodic, partial relaxation of quantum wells and barriers is observed with both plastic and elastic components leading to basis and prismatic stacking faults, which create planar clusters over tens of nanometres in size.

Another property which influences the strain relaxation process in SL is the initial strain state of the substrate. The latter has little representation in the literature. Therefore, the influence of the residual strain of the substrate on the structural properties of SL is not yet fully understood. In our work, we investigated the strain and relaxation of variety GaN/AlN SLs grown on different templates. We study the influence of strain in buffer/template systems on the structural perfection of the SL structures, i.e. layer thickness, radius of curvature, density of dislocations and density of cracks.

2. Experimental details

In order to create differently strained systems, SLs were grown on structurally different templates ($5 \mu\text{m}$ MOCVD GaN on c -sapphire and 340 nm AlN on c -sapphire; hereafter referred to as the GaN and AlN templates, respectively). The GaN template is known to be virtually strain free, i.e. possessing the bulk GaN lattice constant, while the much thinner AlN template demonstrates a small amount of residual strain during

the growth on sapphire. A buffer layer consisting of a 224 nm layer of undoped GaN followed by a 180 nm layer of Si-doped GaN for a bottom electrical contact was grown on each template. Then, one series of 30 period GaN/AlN SLs was grown on GaN templates and another on AlN templates. The specific thickness for each SL layer is presented in table 1. All GaN layers of the SLs were doped with Si ($2 \times 10^{18} \text{ cm}^{-3}$), and finally the SLs were capped by 180 nm layer of Si-doped ($2 \times 10^{18} \text{ cm}^{-3}$) GaN for a top electrical contact [12]. The samples were grown at 760°C , under an activated nitrogen plasma flux which is calibrated to grow in a nitrogen-limited regime at 0.26 ML s^{-1} . The mass fluxes in monolayers per second (ML s^{-1}) have been deduced from reflection high-electron energy diffraction (RHEED) intensity oscillations at low temperature to prevent a possible underestimation due to metal desorption.

The SLs in our study were examined by (0002) ω - 2θ scans and (11–24) reciprocal space mapping (RSM) using high-resolution x-ray diffraction (HRXRD) on a PANalytical X’Pert PRO MRD. The strain in the buffer layers was determined from the analysis of wide-angle scans, i.e. from the angular separation between (0002) reflection from GaN or AlN and (0006) reflection from the sapphire substrate. Radius of curvature of the samples was determined by measuring the deviation of the angle of sapphire XRD reflection across the sample [13].

Analysis of the shape of different reciprocal lattice points using RSMs and ω -scans allows identifying characteristic features associated with different defect types. In particular, the vertical microstrain (typically arising from strain gradients or from strain fluctuations around crystal defects) and the vertical size of coherently diffracting domains can be found by analysing ω - 2θ scan peak widths, whereas the mosaic tilt, lateral microstrain, and lateral size of coherently diffracting domains can be found from ω -scan peak widths. For c -plane layers this analysis is typically performed using Williamson–Hall plots of the (0001) series of reflections. From the 2θ - ω and ω -scans as a function Williamson–Hall plots on the reflection order, the vertical and lateral correlation lengths and tilt were obtained. The density of screw-type dislocations of GaN layers was calculated from the tilt angle. For the calculation of the density of edge-type dislocations, the twist angle was determined from a series of scans of asymmetrical reflections with increasing lattice plane inclination.

The elastic strain distribution in the structure over its thickness was determined according to [14]. For multilayered

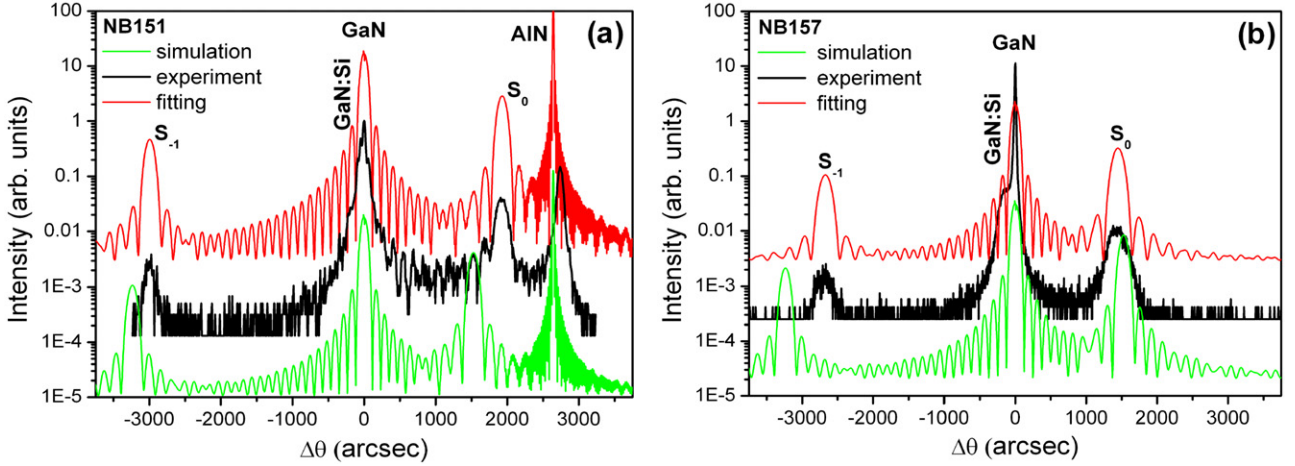


Figure 1. HRXRD ω - 2θ scans of GaN/AlN SLs grown on (a) AlN (NB 151) and (b) GaN (NB 157) templates. Green—simulation, black—experiment, red—fitting.

structures the position of the neutral plane and the wafer radius of curvature can be calculated in a similar way as described for the single-layer system. The strain ε_i in the i th layer at the position z along the c -axis is calculated by equation (1),

$$\varepsilon_i = \frac{d_{l0}}{d_{li}} \cdot \left(1 + \frac{z + h_0 - w}{R} \right) - 1, \quad (1)$$

where w is the distance between the neutral plane and the bottom of the substrate, d_{l0} represents the lattice constant of the substrate at the neutral plane, d_{li} is the lattice constant in the i th layer, h_0 the thickness of the substrate, and R is radius of curvature of the system. For the substrate $i = 0$ is used and for successive layers above, $i = 1, 2, 3 \dots$.

If, however, the layer contains misfit dislocations we recommend to use effective lattice constant as proposed in [15], and given by equation (2),

$$d'_{l1} = d_{l1} + \frac{N_1 - N_0}{N_0} \cdot b_1, \quad (2)$$

where d'_{l1} represents the effective lattice constant, d_{l1} the lattice constant calculated using Vegard's law, N_1 and N_0 are the number of atoms along each side of the interface between the layer and the substrate, respectively, and b_1 is the component of the Burgers vector along the interface. This effective lattice constant should then be used instead of d_{l1} for all following calculations.

The radius of curvature R of the multilayered structure was calculated by using equation (3),

$$R = -\frac{N}{D}, \quad (3)$$

where numerator N and denominator D can be expressed as a complex equation that contains elastic constants, thicknesses and lattice parameters of layers [15].

Comparing the dislocation density with the corresponding strain ε_i , it is possible to calculate the dislocation contribution to the extra bending. According to the results of [15] this relation can be presented in the form:

$$\varepsilon_i = \left(\frac{\Delta a_i}{a} \right)_\perp = \left(\frac{1+\nu}{1-\nu} \right) \left(\frac{\Delta a}{a} \right)_{\text{rel}} - \frac{2\nu}{1-\nu} \cdot \rho_i b_i, \quad (4)$$

where ρ_i is misfit dislocation density associated with the interface between i th and $(i-1)$ th layers and b_i is the component of the Burgers vector parallel to the interface, ν is the Poisson coefficient.

Diffraction rocking curves were simulated with the plane-waves method [16] that is quite adequate for planar structure and gives the same result as Takagi-Taupin approach [17]. Wave vectors in the crystal were calculated numerically [18]. Azimuthal scanning was simulated by changing the misorientation angle of GaN layers and the miscut angle of the substrate. The results obtained were checked by native 3d modelling with the help of the improved n -beam modelling technique proposed in [19] and described in detail in [20]. The lattice constant (a), Young's modulus (E), and Poisson ratio (ν) of Al_2O_3 [21], GaN and AlN [22] were used for calculation of the radius of curvature.

3. Results and discussion

The HRXRD ω - 2θ scans of the symmetrical 0002 Bragg reflection of the two GaN/AlN SLs grown on different templates together with a simulation and fitting curves are shown in figures 1(a) and (b). Along with the substrate peak (GaN) and the main peak caused by the averaged lattice structure (S_0 is zeroth-order satellite), one can observe the complex interference structure at the rocking curve tails, the so-called 'satellite structure'. Satellite peaks, up to third orders, are observed in all cases. The distance between observed satellite peaks is related to the multilayer periodicity (T) of the structure. The results obtained evidence sharp interfaces of the multilayered structure and well-defined periodicity. It is important to note that symmetrical (0002) reflection is only sensitive to the lattice strain perpendicular to the layers.

The period T and the average interplanar spacing (d) are obtained immediately from ω - 2θ scan of SL. The period T is determined by spacing between two satellites $\delta\theta$:

$$T = \frac{|\gamma_\lambda| \cdot \lambda}{\sin(2\theta_B) \cdot \delta\theta}, \quad (5)$$

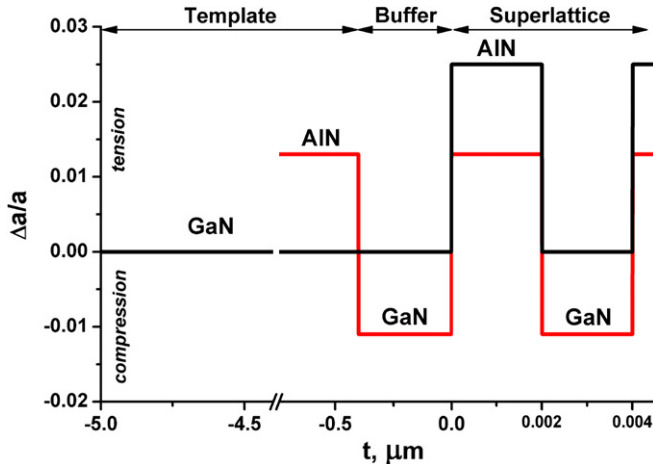


Figure 2. Thickness distribution of in-plane strain in GaN/AlN SLs grown on the AlN template (red line) and the GaN template (black line).

while $\langle d \rangle$ from the angle between the GaN peak and central peak of SL (zeroth-order satellite) $\Delta\theta$:

$$\varepsilon_{\text{aver}} = \frac{\langle d \rangle - d_0}{d_0} = -\Delta\theta / \left(\tan(\theta_B) \cdot \frac{2|\gamma_h|}{\gamma_0 + \gamma_h} \right), \quad (6)$$

where d_0 is the interplanar spacing of GaN (0 0 0 2), γ_0 and γ_h denote the direction cosines of the primary and diffracted waves in the Bragg maximum with respect to the internal surface normal.

Detailed analysis of the SLs parameters has been done through calculations of the XRD rocking curves for all structures by using the relations of dynamical diffraction theory. The technological parameters of the structures were used as initial conditions for simulation of the rocking curve spectra. As a result visible deviation of simulated peaks with respect to experimentally measured ones is observed (see figure 1). This demonstrates a difference in the SL-layers' thickness predicted from the technological growth parameters from their real thickness. Indeed, fitting the theoretical HRXRD spectra to the experimental data yields structural parameters that considerably differ from technological ones (see table 1).

The residual strain of the samples acts to bend the whole sample, macroscopically deforming it and influencing the growth process [9, 23]. In order to understand the effect of this on our samples, we analysed the in-plane strain and the induced curvature for an ideal, dislocation-free structure grown on different templates. Using equation (1), we have calculated the variation of ideal in-plane strain along the growth direction for different templates taking into account their partial relaxation (see figure 2). This partial relaxation is demonstrated in the radius of curvature. The calculated values of the radii with equation (3) for the non-relaxed system (R_1) are considerably less than those measured experimentally ($R_{\text{exp.}}$) for both types of template (see table 2) indicating the fact that SL structures are partially relaxed. At the same time the calculated values of the radii for the partially relaxed system (R_2) approach experimentally measured ones. Since, HRXRD φ scans show that the misorientation of the GaN and AlN unit cells with

respect to the substrate plane is $\sim 30^\circ$; the main relaxation mechanism of these structures is the formation of dislocations through the cracking process [2, 9, 23].

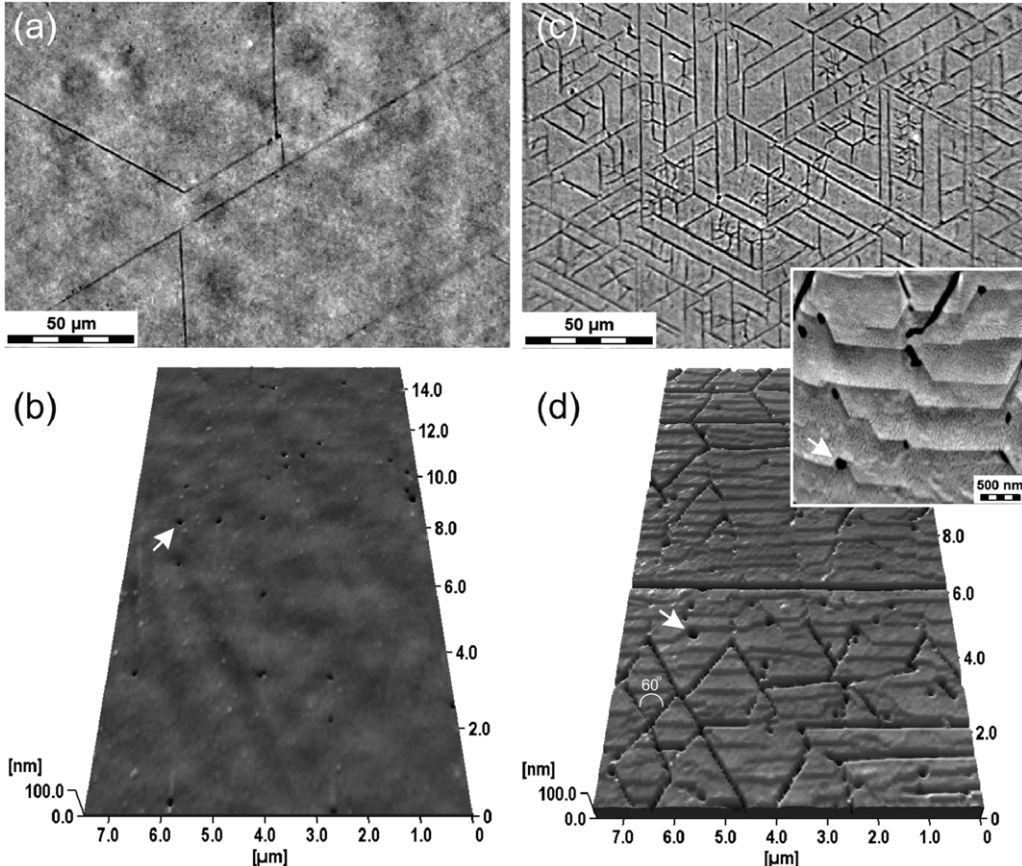
As shown in figure 2 the tensile strain at the GaN-buffer/SL interface is higher for the sample grown on the GaN template compared with the sample grown on the AlN template. This is the stimulus for the formation of cracks predominantly in samples grown on the GaN template. In fact, due to large lattice mismatch between GaN and sapphire ($\sim 16\%$) an epitaxial growth of GaN induces strong compressive stresses in these layers. It is well known that to reduce density of dislocations resulting from this large mismatch GaN layers should be grown thicker than $\sim 1 \mu\text{m}$. As a result, the thick GaN template layer will be fully relaxed as well as the GaN-buffer layer grown on this template. Thus, the first AlN layer of the SL, following the GaN-buffer layer will be under tensile stress due to the lattice mismatch between GaN and AlN (2.5%). Obviously, this increases the risk of crack formation in the SL.

If the template type is changed to a relatively thin AlN layer on sapphire, a different scenario is encountered. The lattice mismatch between AlN and sapphire ($\sim 13\%$) also induces strong compressive stress. However, we found that the AlN template layer is only partly relaxed during the growth. This is confirmed by comparing the experimental AlN peak in the HRXRD spectrum with the simulated peak which is fixed at the bulk AlN Bragg position (see figure 1(a)). The AlN template layer is compressed along the c -axis and tensile strained of about 0.32% in the perpendicular direction. The AlN template layer and the GaN-buffer layer have similar thickness ($\sim 400 \text{ nm}$) and strain (tensile-AlN, compressed-GaN). Therefore, the strain will be compensated in the buffer/AlN template structure with low residual strain on the GaN-buffer surface. Thus, the first AlN layer, beginning the SL, will be under lower tensile stress than in the case of the GaN template. As a result subsequent SL layers will grow under reduced strains. The strain fields have considerable influence on relaxation mechanisms of subsequent GaN and AlN layers during the growth. The growth on partially relaxed AlN templates yields the crack-free structure with the excess strain relieved by the formation of misfit dislocations. However, for growth on GaN templates, the higher initial strain in the SL layers leads to cracking of the film. In this case the material between the cracks is left with lower density of dislocations.

Typical patterns of cracks and surface morphology of the top layer for SLs grown on different templates are shown in figure 3. It shows the huge difference in the average crack spacing that indicates level of biaxial tensile stress in the epitaxial layers prior to crack nucleation and growth. The linear crack density (N_{cracks}) is significantly greater for the structures grown on GaN templates (see figure 3(c)) and table 1). This is obviously caused by the different strain states of GaN-buffer layers grown on different templates. The relaxation of stressed GaN/AlN SLs grown on the GaN templates results in the formation of misfit dislocations at various interfaces and appearance of cracks. The surface morphology of these samples exhibits a 'step-flow' pattern (see figure 3(d)) indicative of monolayer two-dimensional growth. It must be noted that the shape of these terraces is different

Table 2. Radius of curvature and density of dislocations of GaN/AlN SLs grown on the GaN and AlN templates.

Samples	$R_{\text{exp.}} (\text{m})$	$R_1 (\text{m})$	$R_2 (\text{m})$	$N_{\text{edge}} (\times 10^8 \text{ cm}^{-2})$	$N_{\text{screw}} (\times 10^8 \text{ cm}^{-2})$	$N_{\text{total}} (\times 10^8 \text{ cm}^{-2})$
<i>GaN template</i>						
NB 165	4.06 ± 0.12	0.058	2.04	0.16	1.02	1.27
NB 166	6.25 ± 0.31	0.062	3.62	0.65	1.13	1.87
NB 157	7.50 ± 0.32	0.066	5.46	0.20	1.18	1.40
NB 158	7.60 ± 0.27	0.042	5.02	0.56	0.77	1.42
<i>AlN template</i>						
NB 148	7.50 ± 0.23	0.221	7.02	47.50	0.14	53.7
NB 151	9.90 ± 0.08	0.223	7.93	12.90	0.12	14.1
NB 152	12.7 ± 0.05	0.226	10.1	11.70	0.50	12.4

**Figure 3.** Transmitted light optical microscopy micrographs of microcracks and corresponding 3D AFM images of surfaces in the NB152 (a), (b) and NB166 (c), (d) samples. Enlarged 2D AFM image of growth steps on the NB166 sample is shown in the inset.

from that of cracks. Hence, the cracks observed were formed after the growth process. But, at the same time there are many pin-holes (indicated by white arrows) on both NB152 and NB166 samples' surfaces which stop a 'step-flow'. As described elsewhere, these pin-holes correspond to threading dislocations intersections at the surface. Pin-hole densities are 2.1×10^7 and $3.6 \times 10^7 \text{ cm}^{-2}$ for the NB152 and NB166 samples, respectively. These values are less than threading dislocation density determined by x-ray measurements (5×10^7 and $1.13 \times 10^8 \text{ cm}^{-2}$, respectively). The discrepancy should be caused by the fact that pin-holes are formed by the number of dislocations (from 2 to 10). Moreover, the misfit dislocations do not enter on the surface of the samples. Thus, they are invisible for optics but well registered by x-ray. In general, the total dislocation density (all types of dislocations), measured

similarly to [9, 13, 23] is an order of magnitude higher for SLs on AlN templates (see table 2).

In our case GaN films normally contain threading dislocations of the edge ($b = 1/3(1\bar{1}-2\bar{0})$), mixed ($b = 1/3(1\bar{1}-2\bar{3})$) and screw ($b = (0\bar{0}\bar{0}1)$) types with the line direction along $[0\bar{0}\bar{0}1]$. There are usually less than 2% screw dislocations [24], but the ratio of mixed to edge dislocations is variable. Each dislocation type is associated with a local lattice distortion; for dislocations running along $[0\bar{0}\bar{0}1]$, edge dislocations accommodate a lattice twist, screw dislocations accommodate a lattice tilt and mixed dislocations accommodate both processes [25]. The screw component of dislocations with Burgers vector parallel to the interface and edge dislocations with Burgers vectors $b_E = 1/3(1\bar{1}-2\bar{0})$ result in the twisting of the planes. This is a direct verification

of the theoretical concept. Of course, the dislocation type will alter if the line direction of dislocation changes (while the same Burgers vector is present). These distortions are often approximated by the mosaic model, which assumes that the film consists of perfect blocks which are tilted or twisted with respect to each other (this is less appropriate for films with low dislocation density [25]).

In many cases the effects of various broadening factors on ω scans should be separated and dislocation densities can be calculated. In highly defective III-nitride films lattice twist and tilt are directly related to the dislocation density, lateral correlation lengths and diffuse scattering; although, in principle, the peak broadening also depends on the spatial distribution of dislocations within the film. For wurtzite III-nitrides, screw-type dislocations with a Burgers vector $b = (0\ 0\ 0\ 1)$ result in a tilt of lattice planes, which in turn reflects itself in the full-width at half-maximum (FWHM) of symmetric x-ray scans' rocking curves. However, a majority of dislocations in III-nitrides are of edge type with a Burgers vector $b = 1/3[1\ 1\ -2\ 0]$. Unfortunately, the twist of lattice planes induced by edge-type dislocations is considerably more difficult to measure by HRXRD directly. The in-plane rotation (twist components) of the crystallites of the GaN layer can be extracted from a series of ω scans of asymmetrical reflections using quasi-symmetric configuration (skew geometry) with increasing lattice plane inclination.

The relaxation process of stressed GaN/AlN SLs differs for different templates, which can be seen from asymmetric reciprocal space maps (RSM). Figures 4(a) and (b) show the RSMs for the NB 151 and NB 158 samples, grown on the AlN and GaN templates, respectively. From an analysis of these RSMs we have concluded that the GaN-buffer layer is more relaxed in the case of growth on the GaN template (degree of relaxation $\sim 80\%$), in comparison with the growth on the AlN template (degree of relaxation $\sim 70\%$). Obviously, as it is outlined in figure 4, the GaN template is fully relaxed (the calculated peak position for fully relaxed GaN coincides with the peak position obtained from the experiment). Therefore, the residual strain in the GaN-buffer layer as well as average strain within one period of the SL for samples on the GaN template differs from samples on the AlN template. It can also be seen from the shift of the satellite structure of the SL with respect to surface normal for the structures grown on the AlN and GaN templates (see figure 1).

The intensity distribution of diffuse scattering on asymmetric RSMs from different templates shows different types of defects and distortions of the crystal lattice. Contours of equal intensity around the reflection from the GaN-buffer layer grown on the AlN template are elongated in the direction perpendicular to the diffraction vector H . It has been shown recently that dislocation grids, which are localized on hetero-interface, lead to broadening of diffraction pattern in the direction perpendicular to vector of reciprocal lattice [13, 26]. On the other hand, the intensity distribution around the GaN reflection for samples grown on the GaN template is elongated in the direction perpendicular to the normal of the surface (Q_z -axis) that is correct for reflections obtained in different geometries. This is typical for relation of components of strain

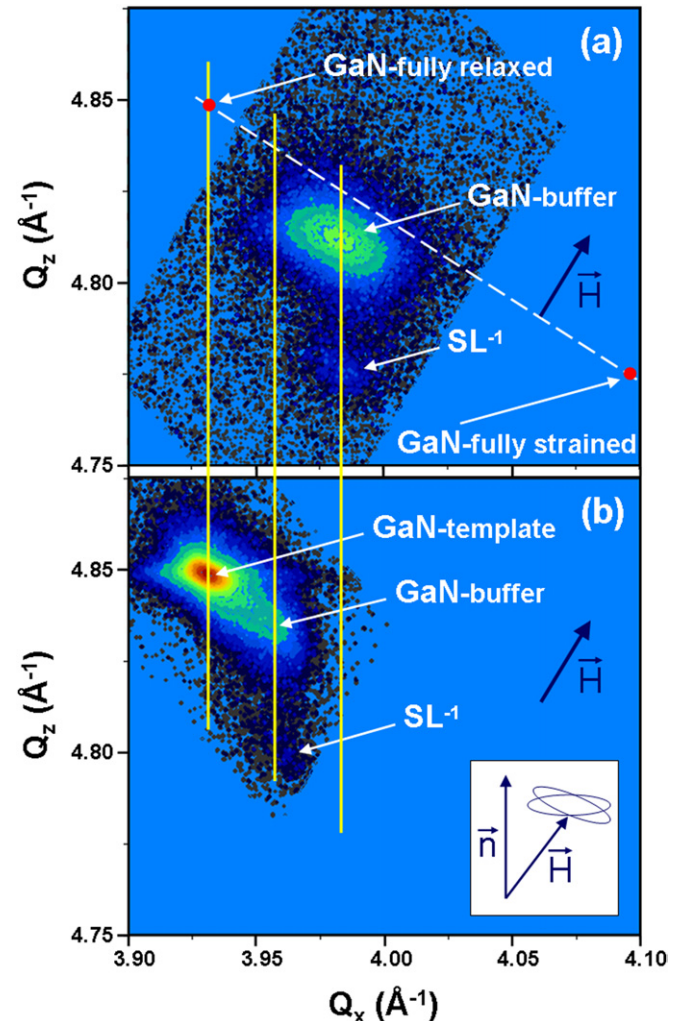


Figure 4. Reciprocal space maps (RSM) around the (11–24) reflection of GaN/AlN SLs grown on the (a) AlN (NB 151) and (b) GaN (NB 158) templates. Dashed line—line of GaN relaxation. Q_z and Q_x are the reciprocal space coordinates, which are perpendicular and parallel to the surface. H —vector of diffraction.

tensor $\langle \varepsilon_{xx} \rangle > \langle \varepsilon_{zz} \rangle$ and corresponds to stronger local variation of distance between planes normal to the surface than between planes parallel to the surface.

Characteristic ratios between the components of microdistortion ($\varepsilon_{xx} > \varepsilon_{zz}$) are observed for all samples, which points out the prevalent density of threading dislocations of both screw and edge type (or mixed dislocations). Thus, one can see a different character of dislocation structure changing for structures grown on different templates. It leads us to suggest different relaxation mechanisms in these structures. In the case of AlN templates, relaxation is likely caused by bending of threading dislocations or by an accumulation of a network of dislocations. As for the samples grown on GaN templates, relaxation occurs by independent 3D, island growth in the AlN layer (with subsequent coalescence of islands), which can be connected with the generation of new threading edge dislocations. These mechanisms, in general, are described in the literature as plastic and elastic mechanisms.

The parameters obtained from fitting HRXRD curves for all SLs are given in table 1 as the experimental values and

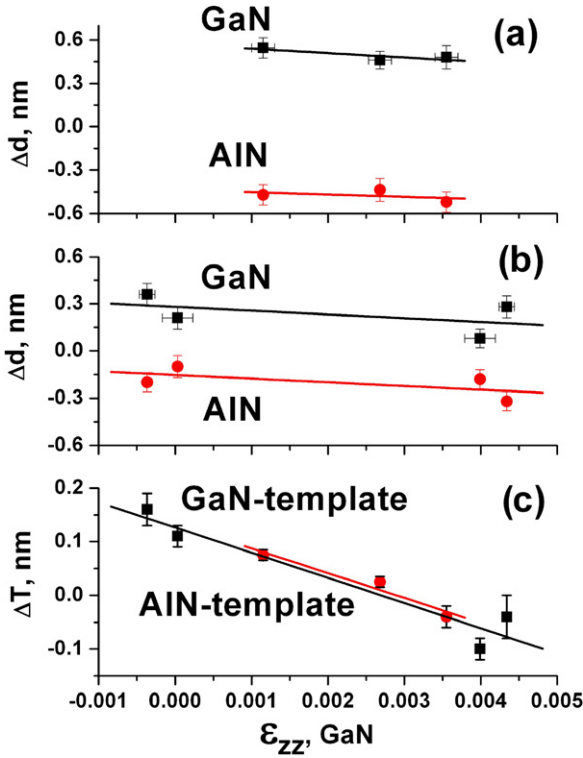


Figure 5. The differences in thickness (Δd) of SL-layers grown on the AlN (a) and GaN (b) templates, and differences in SL periods (ΔT) for both templates (c) as a function of the strain in the GaN-buffer layer.

compared with the values obtained from the technological growth parameters. Significantly, we find from examining these data that there is a discrepancy between the layer parameters as given from the technological growth and the fitted rocking curve for all SLs. If we define the difference $\Delta d = d_{\text{techn}} - d_{\text{exp}}$, where d_{techn} is the technological or designed thickness and d_{exp} is the experimental or measured thickness (from the fitting) of the SL layers, then we can look at the dependence of Δd on the out-of-plane strain (ϵ_{zz}) of the GaN-buffer layers to gain an understanding of the different configurations. These trends are plotted for the growth on the AlN and GaN templates in figures 5(a) and (b), respectively. Despite the similar behaviour (thinning of GaN and thickening of AlN layers) the dependences of Δd on strain in the GaN-buffer layer differs significantly for structures grown on the different templates. The magnitude of the thinning or thickening is larger for structures grown on the AlN templates than for structures grown on the GaN templates. Figure 5(c) shows that the dependence of the period difference, $\Delta T = T_{\text{techn}} - T_{\text{exp}}$ (T_{techn} is technological and T_{exp} is experimental data of SL periods), on strain in the GaN-buffer layer is linear and evidently independent of the specific templates used. Notably, after extrapolation, the strain value at which $\Delta T = 0$, i.e. where there is no change in period from the expected growth parameters to the measured value, is not at zero strain. In addition, we find that the average strain along the growth direction ($\epsilon_{\text{aver.}}$) within one period of the SL, calculated as a weighted average of strain in the layers [27], is not equal to the strain (ϵ_{zz}) in the GaN-buffer

layers (table 1). The average strain was calculated using the formula $\epsilon_{\text{aver.}} = (\varepsilon_1 t_1 + \varepsilon_2 t_2)/(t_1 + t_2)$, where ε_1 , t_1 and ε_2 , t_2 are the averaged values of strain and thickness of GaN and AlN layers of SL, respectively. The data are very close to values calculated with equation (6) that evidences good correlation of results obtained by different methods.

An unaccounted-for thinning of GaN layers during the growth of an AlN cap layer was also shown in [28]. They explain this fact by GaN decomposition due to an exchange mechanism between the Al atoms from the cap layer and the Ga atoms from the GaN layers and show that this phenomenon is thermally activated ($> 720^{\circ}\text{C}$). It is important to note that we did not observe any alloying of AlN and GaN at the interfaces as previously reported [29]. This result indicates that the growth temperature (760°C) of the AlN barriers was low enough not to cause significant interdiffusion with the GaN wells which could also result in a reduction in the apparent GaN well thickness, but it is sufficient for GaN decomposition resulting from Al/Ga exchange. Therefore, the Al/Ga exchange results not only in GaN thickness reductions but also in an increase in AlN thickness for all SLs. Obviously, the exchange between Al adatoms and Ga atoms from the GaN layers occurs during the deposition of AlN on the GaN. Indeed, this process of replacement of a Ga atom from the first layer with an Al adatom is energetically more favourable, compared with the occupation of sites on the top of the layer by an N atom [30]. The energy barrier for diffusion of this new Ga adatom is just 0.27 eV, much lower than in the case of the Al adatom on the surface.

From this fact, that the layers of the SLs were deposited under similar conditions, but their parameters differ from technological ones, we proposed that the strain field of the template/buffer system influences the Al/Ga exchange. Thus, the Al/Ga exchange depends also on the strain state of the structures and different magnitudes of the thinning/thickening of SL layers for different templates can be explained by relaxation processes in these structures. Indeed, as one can see from table 1, the density of cracks is inversely proportional to the strain in the buffer. That fact let us conclude that during the process of cracking there is a significant redistribution of stress with the relaxation of the system. This seems to lead to the growth rates of the SL layers being more correlated with the technological parameters for the structures with the GaN template, i.e. Δd is closer to zero as depicted in figure 5.

According to the values of the radii of curvature presented in table 2 we can assume that both systems are equally relaxed. As the data of other authors [23] testify, the amplitude of a deformation jump (the radius of curvature) depends on the law of dislocation distribution in the layers [23]. Our calculations showed that taking this factor into account does not change the radius of a system bending significantly. Hence, we see that the dislocation influence alone cannot explain the large discrepancy in the system bending.

According to [31] the layer thicknesses of both of our SL systems do not exceed the critical value for relaxation due to dislocation formation. In this case the relaxation by twist in the SL layer, as described in [9], is not applicable, because the cell rotations of GaN and AlN are only 30° for

both template systems. At the same time spontaneous change of the layers thickness should be one of the relaxation channels. Moreover, due to the reduced diffusion length of Al compared with Ga atoms and to its enhanced incorporation probability, the role of dislocations in the Al/Ga exchange processes is very crucial.

It is important to point out that the above described unintentional changes in the thickness of the SL barriers and wells considerably affect the position of the GaN/AlN SLs' electronic miniband. This result should be taken into account when designing photonic structures.

4. Conclusions

In conclusion, the results of this work can be stated as follows: there is a strong dependence of parameters of the overgrown structure on the initial strain state of the template/buffer system (i.e. template type). The strain fields considerably influence the growth rates and relaxation mechanisms of subsequent GaN and AlN layers during the growth. Structural perfection of the SL structures is strongly dependent also on the initial strain state of the template/buffer system. We find that for growth on partially relaxed AlN templates, the crack-free structure is formed with the excess strain relieved by the formation of misfit dislocations. However, for growth on GaN templates, the higher initial strain in the SL layers leads to cracking of the film. In this case the material between the cracks is left with lower density of dislocations. This results in a compromise being made for device quality. If large area devices are needed the growth on AlN templates may be preferred with a slight loss in quality due to dislocations. If smaller area devices are acceptable it is preferable to use GaN templates as substrates. In this case a small area of material may be chosen to be crack free with the highest possible performance.

Acknowledgments

The authors acknowledge the financial support of the NSF (through Grant DMR-0520550), National Academy of Sciences of Ukraine (Grant No 4/08-H), Ministry of Education of Ukraine (Project No M90/2010) and Russian-Ukrainian program 'Nanophysics and nanotechnology'.

References

- [1] Morkoç H 2008 *Handbook of Nitride Semiconductors and Devices* (Berlin: Wiley-VCH)
- [2] Einfeld S, Heinke H, Kirchner V and Hommel D 2001 *J. Appl. Phys.* **89** 2160
- [3] Nicolay S, Feltin E, Carlin J F, Grandjean N, Nevou L, Julien F H, Schmidbauer M, Remmelle T and Albrecht M 2007 *Appl. Phys. Lett.* **91** 061927
- [4] Bayram C, Pétré-laperne N, McClintock R, Fain B and Razeghi M 2009 *Appl. Phys. Lett.* **94** 121902
- [5] Ma Z F, Zhao D G, Wang Y T, Jiang D S, Zhang S M, Zhu J J, Liu Z S, Sun B J, Yang Hui and Liang J W 2008 *J. Phys. D: Appl. Phys.* **41** 105106
- [6] Kandaswamy P K *et al* 2008 *J. Appl. Phys.* **104** 093501
- [7] Daudin B, Widmann F, Feuillet G, Samson Y, Arlery M and Rouvière J L 1997 *Phys. Rev. B* **56** R7069
- [8] Mula G, Adelmann C, Moehl S, Oullier J and Daudin B 2001 *Phys. Rev. B* **64** 195406
- [9] Kladko V P, Kuchuk A V, Safryuk N V, Machulin V F, Belyaev A E, Hardtdegen H and Vitusievich S A 2009 *Appl. Phys. Lett.* **95** 031907
- [10] Marée P M J, Barbour J C, van der Veen J F, Kavanagh K L, Bulle-Lieuwma C W T and Viegers M P A 1987 *J. Appl. Phys.* **62** 4413
- [11] Kandaswamy P K, Bougerol C, Jalabert D, Ruterana P and Monroy E 2009 *J. Appl. Phys.* **106** 013526
- [12] DeCuir Jr E A, Fred E, Passmore B S, Muddasani A, Manasreh M O, Xie J, Morkoç H, Ware M E and Salamo G J 2006 *Appl. Phys. Lett.* **89** 151112
- [13] Kladko V P *et al* 2009 *J. Appl. Phys.* **105** 063515
- [14] Dieing T and Usher B F 2003 *Phys. Rev. B* **67** 054108
- [15] Chu S N G, Macrander A T, Strege K E and Jognston W D Jr 1985 *J. Appl. Phys.* **57** 249
- [16] Bartels W J, Hornsra J and Lobeek D J W 1986 *Acta Crystallogr. A* **42** 539
- [17] Authier A 2001 *Dynamical Theory of X-Ray Diffraction* (New York: Oxford University Press)
- [18] Yefanov O M and Kladko V P 2006 *Metallofiz. Noveish. Tekhnol.* **28** 227
- [19] Stetsko Yu P and Chang S-L 1997 *Acta. Crystallogr. A* **53** 28
- [20] Yefanov O M, Kladko V P and Machulin V F 2006 *Ukr. J. Phys.* **51** 895
- [21] http://www.mt-berlin.com/frames_cryst/descriptions/sapphire.htm
- [22] <http://www.ioffe.ru/SVA/NSM/Semicond/>
- [23] Kladko V P, Safryuk N V, Kuchuk A V, Machulin V F and Belyaev A E 2009 *Ukr. J. Phys.* **54** 014
- [24] Srikant V, Speck J S and Clarke D R 1997 *J. Appl. Phys.* **82** 4286
- [25] Liu B *et al* 2008 *J. Appl. Phys.* **103** 023504
- [26] Ratnikov V V, Kyutt R N, Shubina T V, Paskova T and Monemar B 2001 *J. Phys. D: Appl. Phys.* **34** A30
- [27] Mazur Yu I, Wang Zh M, Salamo G J, Strelchuk V V, Kladko V P, Machulin V F, Valakh M Ya and Manasreh M O 2006 *J. Appl. Phys.* **99** 023517
- [28] Gogneau N, Jalabert D, Monroy E, Sarigiannidou E, Rouviere J L, Shibata T, Tanaka M, Gerard J M and Daudin B 2004 *J. Appl. Phys.* **96** 1104
- [29] Schulze F, Blasing J, Dadgar A and Krost A 2003 *Appl. Phys. Lett.* **82** 4558
- [30] García-Díaz R, Cocoletzi G H and Takeuchi N 2010 *J. Cryst. Growth* **312** 2419
- [31] Bykhovski D, Gelmont B L and Shur M S 1997 *J. Appl. Phys.* **81** 6332